ANALYSIS OF VIBRATION MODES OF SEMI-TRAILER AXLE AND THEIR EFFECTS ON FATIGUE LIFE

[1]Kazimierz DROZD, [2]Jonas MATIJOŠIUS, [3]Iryna BORETSKA

[1]Faculty of Mechanical Engineering, Lublin University of Technology, Lublin, Poland, EU, k.drozd@pollub.pl

[2]Mechanical Science Institute, Vilnius Gediminas Technical University, Vilnius, Lithuania, EU, jonas.matijosius@vilniustech.lt

[3]Department of Information Technologies, Ukrainian National Forestry University, Lviv, Ukraine, boretska@nltu.edu.ua

https://doi.org/10.37904/metal.2023.4645

Abstract

During the operation of the axle, the load acting on the axle housing in the vertical direction has a significant effect on the fatigue life of the components. Cracks are caused by a constant stress concentration in the axle housing, resulting in fatigue at the concentration point. If the load exceeds a certain threshold, microscopic cracks will begin to form at the stress concentration point. Later, the cracks grow due to the cyclic load of fatigue. Eventually, the cracks reach a critical limit and then the structure suddenly breaks. Axle housing failures are also affected by factors such as uneven load effect, housing slope, and eccentricity. The paper presents an analysis of reliability and damage to the rear axle of a truck semi-trailer caused by natural vibrations. For this purpose, finite element analysis where conducted, preceded by a theoretical introduction. Several vibration modes were considered in order to determine the most likely point of damage initiation to the semitrailer axle. Comparing the test results with the observations, it was found that natural vibrations in the range of 53-533 Hz may be the cause of the limited fatigue life of the main tube. Due to the greatest deformation of the central part of the axis during vibrations, the greatest stresses in the critical zone will occur for mode 8 at a frequency of about 533 Hz which also means many fatigue load cycles.

Keywords: Natural vibrations, fatigue life, suspension axle, steel

1. INTRODUCTION

Technical issues of road transport safety are widely discussed in the world literature. For example, Rievaj et al. [1] or Dižo and Blatnický [2] studied the behavior of articulated vehicles with different loading conditions under heavy braking conditions. Similar research was also conducted by Šarkan et al. [3]. Vehicle stability studies were also studied by Dizo [2] and Jilek [4]. In turn, the issues of modeling vehicles in motion were dealt with by Vdovin et al. [5]. Research on failures of safety systems in buses was presented by Kilikevičienė et al. [6]. Other studies on the impact of the technical condition of the suspension system were presented in [7]. The durability of the suspension parts refers to the duration of the onset of fatigue, defined as the number of cycles up to a certain component cracking length under cyclic loads [4,6].

In order to reduce the costs of transporting goods, the aim is to increase the amount of cargo transported. This can be achieved, for example, by reducing the curb weight of the vehicle in favor of increasing its payload. However, regulations regarding the axle load on the road surface enforce design changes resulting in an increase in the number of axles. Unfortunately, the disadvantage of such a solution is the deterioration of control and maneuverability of the entire transport set [1,8]. The issue of road transport with a load is presented in the work [7], where the distribution of the center of gravity on the characteristics of the vehicle is presented.

It turns out that the braking system and suspension have a significant impact on the level of road transport safety.

In terms of vehicle stability and traffic safety, the proper technical condition of the chassis assembly of a road transport vehicle plays an important role [9]. For these reasons, this article analyses, based on a numerical model, the strength of the semi-trailer axle of a truck that was damaged during a transport task.

FEM analyzes (finite element method) are widely used in engineering research, mainly regarding the safety of transport by various means of transport [7,10]. Vibrations generated in the suspension of vehicles affect the amplitude and acceleration of the transported load. According to papers [9, 10], the highest spectral density of charge vibrations corresponds to frequencies up to about 50 Hz. Higher frequency vibrations can also be transferred to the load. Source may be road irregularities when the truck is traveling at maximum speed or vibrations generated during braking [11,12].

After axle load during road traffic test, results were published in papers [1,5,13]. Hence, the aim of work was to find whether the natural vibrations could be the cause of damage to the axle in the described critical place.

2. MATERIALS AND METHODS

The structure of the non-driven axle of the car semi-trailer was analysed. In the area marked with a red oval (**Figure 1a**), this axis is sometimes damaged. Local damage to the paint coating is then also visible. This happened that the place of damage is not in the immediate vicinity of the wheel and is even located on the inside of the arm, opposite to the wheel. Damage to the paint coating could have arisen as a result of fatigue deformation of the material surface. The fracture surface has a fatigue character, which leads to the assumption that the damage was caused by cyclical load changes.

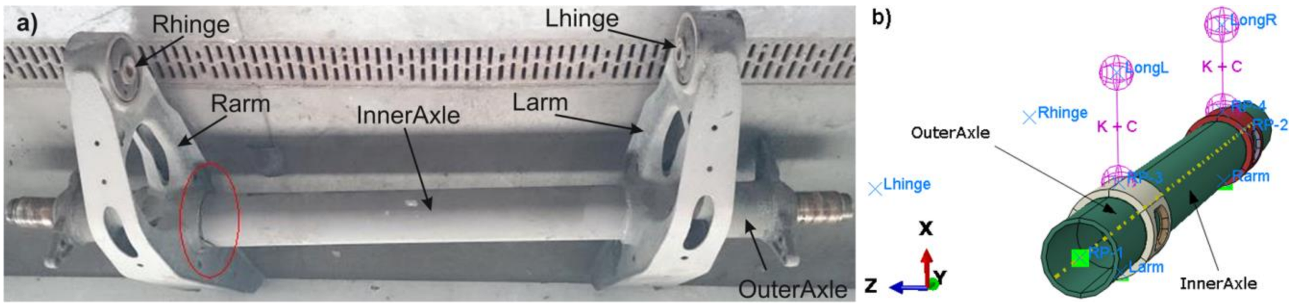

Figure 1 Complete axle with surrounded area of fracture **a)** and model for simulations **b)**. Front in Z direction

In order to verify the thesis on the fatigue nature of the damage, a numerical model of the complete axle was made along with the nearest kinematic nodes (**Figure 1b**). The weight of the solid elements shown in the **Figure 1** is 79 kg, including about 1 kg of the weight of the welds. In addition, the weight of the wheels with brakes (120 kg on one side of the axle) was considered, which was assigned to the RP-1 and RP-2 points. The portion of the weight of the arm, suspension spring and shock absorber contributing to the axle mass was estimated at 25 kg and assigned to Larm and Rarm points. In result the total mass of the model m = 369 kg. The fixed elements of the structure, which had no degrees of freedom, were the points of attachment of the movable suspension elements to the frame (LongL, LongR). Between the Lhinge and Larm points (Rhinge and Rarm as well) a non-deformable arm was included as a rigid body element (not visible in **Figure 1b**), which could rotate around the Y axis at the Lhinge (Rhinge) point.

This model (**Figure 1b**) contains some simplifications in relation to the real structure, among others: the possibility of deformation of the suspension arms, which were modeled with rigid body elements, has been omitted, and it does not consider the stiffness and damping of the road wheels. The wheel was not included in the model because the stiffness of the tire is usually at least 10 times greater than the stiffness of the suspension springs [14,15], and the centre of mass of the wheel normally is in the axis of its rotation (RP-1 and RP-2).

It was assumed that the spring elements of the suspension have a stiffness of K = 4.5 kN·mm^{-1} and the damping coefficient of each shock absorber is C = 10 N·s·mm^{-1} [5,16]. For the axle parts the mesh was created using linear elements of the C3D8R type with reduced integration. As for the number of mesh elements in the simulation (**Figure 1b**), 11,496 elements and 17,943 nodes were assumed for the bushings, and 10,120 elements and 20,424 nodes for the main axle tube. The material properties of all parts made of steel had the following values: Young's modulus 2.04E+11 Pa, Poisson's number 0.3 and density 7.8 Mg·m^{-3}.

The results obtained during the simulations were evaluated in terms of possible errors by comparing some of them with the results of analytical calculations of vibration frequency for mode 1. There was discussed the probability of occurrence of various types of axle damage, including possibility of cracking of the tube which is the axle main part. The results and conclusions obtained during the discussion were also compared with the existing literature reports considering similar problems.

For the first few vibration modes, the possibility of forcing natural vibrations by road unevenness was assessed. It was assumed that the dynamic radius of the wheel r_d = 498 mm [7]. For the limiting velocities of 5 km· h^{-1} and 100 km· h^{-1} [12], it was estimated what part of the rotation (or the number of revolutions) the wheel should make between successive road irregularities for vibrations of the calculated frequency were able to occur.

3. RESULTS AND DISCUSSION

Table 1 contains the results of the FEM natural vibration simulations in order of increasing stiffness of the suspension springs for different vibration modes. Only the frequencies corresponding to mode 1 change significantly depending on the stiffness. For the other modes, especially 3 and next, the results vary minimally, if at all. There is practically no difference in natural frequencies for modes 3, 4, 7 and 8.

Table 1 Frequency of the axle natural vibrations

Left, right or both spring stiffness (N/mm)	Vibration mode							
	1	2	3	4	5	6	7	8
	Frequency (Hz)							
1*	0.364	52.58	148.82	149.15	211.20	275.04	471.71	532.67
1000	11.493	53.47	148.82		211.67	275.73	471.72	532.84
1*, 4500	16.419	54.73	148.82		212.23	276.61	471.72	533.05
4400	23.899	56.33	148.83		213.26	278.05	471.72	533.42
4500	24.163	56.41	148.83		213.31	278.12	471.72	533.43
4600	24.424	56.49	148.83		213.36	278.19	471.72	533.45

1* - minimal stiffness, but not requiring model changes

If the stiffness of the suspension springs were not taken into account (1*), the natural frequency for mode 1 would be 0.364 Hz (**Table 1**). This means that even when driving at a speed of 5 km/h, it would be enough for the excitations to be placed on the road every 3.82 m for mode 1 resonance vibrations to occur. Such vibrations consist in equal deflection of both suspension springs simultaneously. For the dynamic radius of the wheel r_d = 498 mm, its dynamic circumference is L_d = 3129 mm. The excitations could therefore be placed in the path every 1.22 revolutions of the wheel of this axle to generate mode 1 vibrations when the vehicle is moving at a speed of only 5 km/h. It does not matter that the tires would not be pressed against the road surface. Although there is no clear information that the simultaneous failure of the suspension springs (resulting in a decrease in stiffness to 0.0 N/mm) took place, this possibility cannot be completely ruled out either.

The analysis was also carried out for the case when the stiffness of each of the suspension springs is reduced (in relation to the nominal one) to K = 1.0 kN·mm^{-1}. The first natural frequency was then 11,493 Hz. Both suspension springs are evenly deflected, therefore the equivalent stiffness of the system is twice as high as the stiffness of one spring. Vibration frequency which is calculated from the formula:

$$f = \frac{1}{2 \cdot \pi} \cdot \sqrt{\frac{2 \cdot K}{m}} \tag{1}$$

where:

f - the frequency of vibrations (Hz)

K - the stiffness of one suspension spring (N·m^{-1})

m - the mass of the vibrating axle assembly (kg)

was f = 11.717 Hz. This means that the difference between the simulation result and the calculation was less than 2 %. For stiffness K = 4.5 kN·mm^{-1}, the frequency calculated from the formula (1) f = 24.856 Hz, which means less than 3 % difference compared to the value of 24.163 Hz given in **Table 1**. Both these differences are acceptable because whole axle during simulation additionally rotates (makes rotational vibrations) round points described Lhinge and Rhinge (**Figure 1**).

Although mode 1 vibrations are most likely to occur, they do not deform the axis in the damage zone (**Figure 1a**). Similarly, the deformation for modes 3 and 4 is only deflection of the outer zone of the axle. The deformation of the part of the axle that cracks occur for mode 2 (**Table 2**, **Figure 2**) and then modes 5-8.

Table 2 contains a summary of the greatest displacement of the axle during natural vibrations for various stiffness of the suspension springs and various modes of deformation. The deformation is mainly in the x direction (U1), but for mode 7 it is in the z direction (U3). For modes 3 and 4, the deformation occurs primarily in the y-z plane, but the magnitude (U) is included in the table. The stiffness (stiffness distribution) of the suspension springs only slightly affects the largest deformation value during vibration.

Table 2 Characteristic displacement values of axle during few first vibration modes

<table>
<tr><th rowspan="5">Left, right or both spring stiffness (N/mm)</th><th colspan="13">Vibration mode and (Figure number)</th></tr>
<tr><th>1</th><th colspan="2">2 (2a)</th><th>3</th><th>4</th><th colspan="2">5 (2b)</th><th colspan="2">6 (2c)</th><th colspan="2">7 (2d)</th><th colspan="2">8 (2e)</th></tr>
<tr><th colspan="13">Displacement in direction (mm)</th></tr>
<tr><th>U1</th><th colspan="2">U1</th><th>U</th><th>U</th><th colspan="2">U1</th><th colspan="2">U1</th><th colspan="2">U3</th><th colspan="2">U1</th></tr>
<tr><th>|min|, max</th><th>min</th><th>max</th><th>max</th><th>max</th><th>min</th><th>max</th><th>min</th><th>max</th><th>min</th><th>max</th><th>min</th><th>max</th></tr>
<tr><td>1*</td><td>1.90</td><td>-1.97</td><td>1.97</td><td>2.16</td><td>2.16</td><td>-3.88</td><td>1.34</td><td>-3.21</td><td>3.21</td><td rowspan="6">-7.78</td><td rowspan="6">0.02</td><td>-7.07</td><td>2.22</td></tr>
<tr><td>1000</td><td>1.89</td><td>-1.97</td><td>1.97</td><td>2.16</td><td>2.16</td><td>-3.90</td><td>1.34</td><td>-3.21</td><td>3.21</td><td>-7.06</td><td>2.22</td></tr>
<tr><td>1*, 4500</td><td>2.04</td><td>-1.79</td><td>2.14</td><td>2.17</td><td>2.17</td><td>-3.91</td><td>1.37</td><td>-3.27</td><td>3.16</td><td>-7.06</td><td>2.24</td></tr>
<tr><td>4400</td><td rowspan="3">1.87</td><td rowspan="3">-1.98</td><td rowspan="3">1.98</td><td rowspan="3">2.16</td><td rowspan="3">2.16</td><td rowspan="3">-3.94</td><td rowspan="3">1.32</td><td rowspan="3">-3.23</td><td rowspan="3">3.23</td><td rowspan="3">-7.05</td><td rowspan="3">2.23</td></tr>
<tr><td>4500</td></tr>
<tr><td>4600</td></tr>
</table>

1* - minimal stiffness, but not requiring model changes

For the higher frequency of natural vibrations, the larger deflections there were also calculated. For mode 2, the deflections are small and symmetrical about the x-axis (**Figure 2a**), except in the case of unequal spring stiffness (row 1*, 4500 in **Table 2**). However, for the fifth and subsequent vibration frequencies, the deformations are much larger and asymmetric (except for the sixth). The theory of elasticity shows that in nodes where the deformation during vibrations is small, the stresses are correspondingly higher [4,17]. In addition, the higher the vibration frequency, the greater the number of fatigue cycles stressing the material. This means that there may be a large effect of natural vibrations according to mode 5-8 and mode 2 on limiting the fatigue life of the critical area of the axle structure (**Figure 1a**).

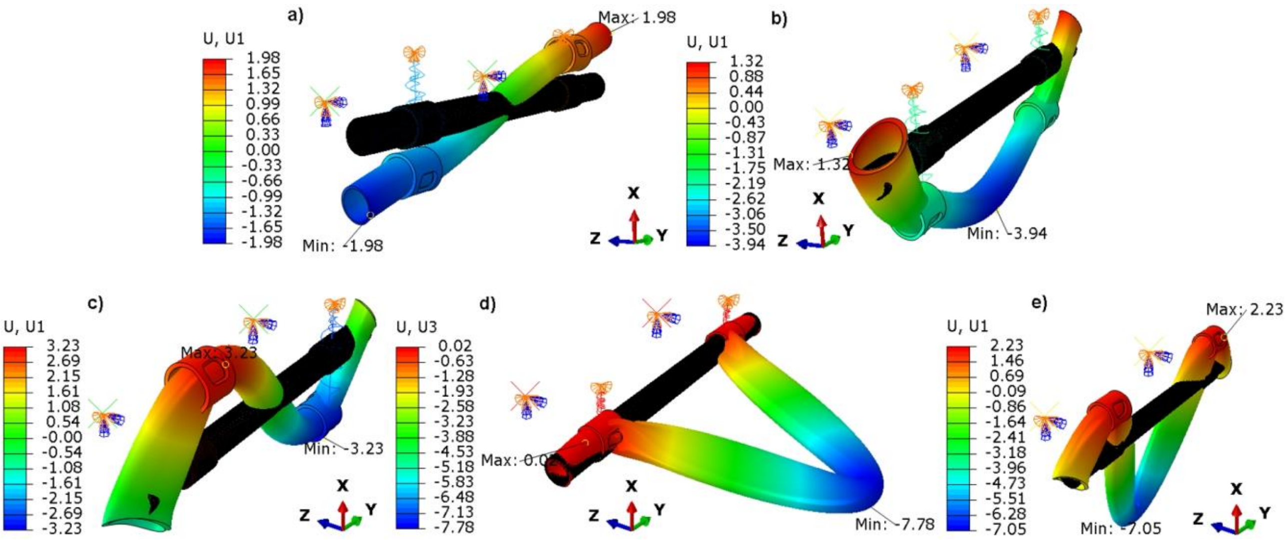

Figure 2 Displacement (mm) in main direction in relation to undeformed (black) axle for spring stiffness 4.5 kN·mm^{-1} and vibration modes: **a)** 2; **b)** 5; **c)** 6; **d)** 7; **e)** 8. Deformation scale factor 150x. Front in Z direction.

Comparing the test results with the observations, it was found that natural vibrations in the range of 53-533 Hz may be the cause of the limited fatigue life of the main tube in the critical zone. Due to the greatest deformation of the central part of the axis during vibrations, the greatest stresses in the critical zone will occur for mode 8 at a frequency of about 533 Hz (**Figure 2e**). It should be noted that many material fatigue load cycles are generated even in a short time of vibration occurrence. Slightly less deformation of the axis and lower stresses from the middle of its part will occur for mode 7 (**Figure 2d**) and even less for mode 6 (**Figure 2c**). For modes 2 (**Figure 2a**) and 5 (**Figure 2b**), the stress values at the critical point (**Figure 1a**) should be lower, due to smaller deformations, and at the same time, the number of fatigue cycles during vibrations is also lower. As in the publication [5] it can be concluded the considered part of the axle may be characterized by a lower fatigue life than its other parts.

4. CONCLUSION

It has been proved that the construction of the tested axle is such that its cracking may occur as a result of stresses caused by natural vibrations of the system with a frequency in the range of (53-533) Hz. Modes of natural vibration causing the greatest fatigue load on the axle are mode 5-8 and mode 2. Mode 1 causes only uniform deformation of the suspension springs, and modes 3 and 4 consist in bending only the outer parts of the axle from the side of the wheels. So, out of the first 8 modes of natural vibrations, only three do not cause the fatigue load of the part of the axle for which cracking was observed. For this reason alone, it can be concluded that the considered part of the axle may be characterized by a lower fatigue life than its other parts. The probability of damage to the axle at the indicated location is increased due to two-thirds more modes of natural vibrations causing local strain of the material here compared to the outer part of the axle.

REFERENCES

[1] RIEVAJ, V., VRABEL, J., SYNAK, F., BARTUSKA, L. The effects of vehicle load on driving characteristics. *Advances in Science and Technology - Research Journal*. 2018, vol. 12, pp. 142-149. Available from: https://doi.org/10.12913/22998624/80896.

[2] DIŽO, J., BLATNICKÝ, M. Investigation of ride properties of a three-wheeled electric vehicle in terms of driving safety. *Transportation Research Procedia*, 2019, 40, pp. 663–670. Available from: https://doi.org/10.1016/j.trpro.2019.07.094.

[3] ŠARKAN, B., JAŚKIEWICZ, M., KIKTOVA, M. The impact of the truck loads on the braking efficiency assessment. *Open Engineering*. 2020, vol. 10, pp. 105–112. Available from: https://doi.org/10.1515/eng-2020-0014.

[4] JILEK, P., BERG, J., TCHUIGWA, B.S.S. Influence of the Weld Joint Position on the Mechanical Stress Concentration in the Construction of the Alternative Skid Car System's Skid Chassis. *Applied Science*. 2022, vol. 12, no. 397, pp.1-19. Available from: https://doi.org/10.3390/app12010397.

[5] VDOVIN, D., LEVENKOV, Y., CHICHEKIN, I. Prediction of fatigue life of suspension parts of the semi-trailer in the early stages of design. In: *IOP Conference Series: Materials Science and Engineering*, Design Technologies for Wheeled and Tracked Vehicles. Moscow, Russian Federation. 2020, vol. 820, 012002. Available from: https://doi.org/10.1088/1757-899X/820/1/012002.

[6] KILIKEVIČIENĖ, K., SKEIVALAS, J., KILIKEVIČIUS, A., PEČELIŪNAS, R., BUREIKA, G., The analysis of bus air spring condition influence upon the vibration signals at bus frame. *Eksploatacja i Niezawodnosc – Maintenance and Reliability*. 2015, vol. 17, pp. 463-469. Available from: https://doi.org/10.17531/ein.2015.3.19.

[7] JURECKI, R., JAŚKIEWICZ, M., WDOWSKI, T. Testing the influence of car load and pressure in tyres on the value of damping of shock absorbers specified with the use of the Eusama method. *Diagnostyka*. 2014, vol. 15, pp. 45–50.

[8] MATUSZAK, Z., BARTOSZ, M., BARTA, D. The application of selected network methods for reliable and safe transport by small commercial vehicles. *Management Systems In Production Engineering*. 2016, vol. 23, pp. 198-204. Available from: https://doi.org/10.2478/mspe-09-03-2016.

[9] CABAN J., NIEOCZYM, A., GARDYŃSKI, L. Strength analysis of a container semi-truck frame. *Engineering Failure Analysis*. 2021, vol. 127, pp. 1-12. Available from: https://doi.org/10.1016/j.engfailanal.2021.105487.

[10] WOZNIAK, M., OZUNA, G. SICZEK, K. The Study on the Damage of the Rear-Axle Shaft in a KIA Truck. *Advances in Science and Technology - Research Journal*. 2020, vol. 14, pp. 115-124. Available from: https://doi.org/10.12913/22998624/126508.

[11] LEVESQUE, W., BÉGIN-DROLET, A., LÉPINE, J. Effects of Pavement Characteristics on Rolling Resistance of Heavy Vehicles: A Literature Review. *Transportation Research Record*, 2023, vol. 0, pp. 1-14. Available from: https://doi.org/10.1177/03611981221145125.

[12] ASHRAF, N., BRYANT, D., FIELDHOUSE, J.D. Investigation of Stick-Slip Vibration in a Commercial Vehicle Brake Assembly. *International Journal of Acoustics & Vibration*. 2017, vol. 22, pp. 326-333. Available from: https://doi.org/10.20855/ijav.2017.22.3478.

[13] FYHR, P., HJELM, R., WAHLSTRÖM, J. An Experimental Study of Forced Vibration Influence on Disc Brake Drag Torque in Heavy Commercial Road Vehicles. *Tribology in Industry*. 2022, vol. 44, pp 123-131. Available from: https://doi.org/10.24874/ti.1132.06.21.09.

[14] DECKER, Ž., TRETJAKOVAS, J., DROZD, K., RUDZINSKAS, V., WALCZAK, M., KILIKEVIČIUS, A., MATIJOSIUS, J., BORETSKA, I. Material's Strength Analysis of the Coupling Node of Axle of the Truck Trailer. *Materials*. 2023, vol. 16, pp. 1-17. Available from: https://doi.org/10.3390/ma16093399.

[15] BALLO, F., PREVIATI, G., MASTINU, G., COMOLLI, F. Impact tests of wheels of road vehicles: A comprehensive method for numerical simulation. *International Journal of Impact Engineering*. 2020, vol. 146, 103719. Available from: https://doi.org/10.1016/j.ijimpeng.2020.103719.

[16] CHAUHAN, M., KOTWAL, G., MAJGE, A. Numerical Simulation of Tire and Wheel Assembly Impact Test Using Finite Element Method. In: *Symposium on International Automotive Technology. SAE Technical Paper*, 2015. Available from: https://doi.org/10.4271/2015-26-0186.

[17] BERNAD, C., LASPALAS, A., GONZÁLEZ, D., NÚÑEZ, J.L., BUIL, F. Transport vibration laboratory simulation: On the necessity of multiaxis testing. *Packaging Technology and Science*. 2011, vol. 24, pp. 1-14. Available from: https://doi.org/10.1002/pts.